Fast electron beam heating in solid targets

Rory J. Garland
Supervisors: A. P. L. Robinson(RAL) & M. Borghesi(QUB)

Queens University Belfast

rgarland05@qub.ac.uk

November 13, 2015

Outline

Motivation

- TNSA
- Fast Ignition ICF
- WDM
- Astrophysical Experiments

Applications

TNSA

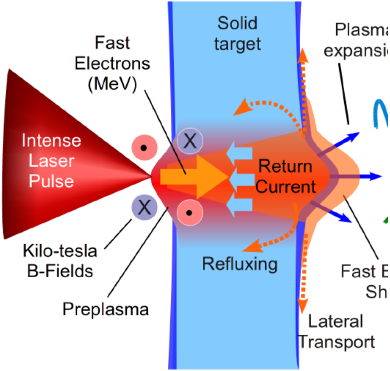

Figure : TNSA

Applications
Fast Ignition

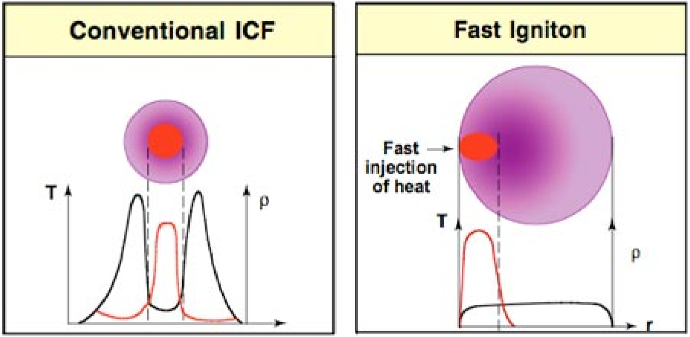

Figure : Direct Drive vs Direct Drive Fast Ignition

What are Fast Electron Beams?

What are Fast Electron Beams?

- Generated from $\mathbf{j} \times \mathbf{B}$ heating.

What are Fast Electron Beams?

- Generated from $\mathbf{j} \times \mathbf{B}$ heating.
- Maxwell-J$\ddot{u}$ttner distribution

What are Fast Electron Beams?

- Generated from $\mathbf{j} \times \mathbf{B}$ heating.
- Maxwell-J$\ddot{u}$ttner distribution
- Temperature scales with:

$$T(MeV) = 0.511\left(\sqrt{1+\frac{I_{18}\lambda_{\mu m}^2}{1.37}}-1\right)$$

What are Fast Electron Beams?

- Generated from $\mathbf{j} \times \mathbf{B}$ heating.
- Maxwell-J$\ddot{u}$ttner distribution
- Temperature scales with:
  $$T(MeV) = 0.511 \left(\sqrt{1 + \frac{I_{18}\lambda^2_{\mu m}}{1.37}} - 1 \right)$$
- Propagate through the target

What are Fast Electron Beams?

- Generated from $\mathbf{j} \times \mathbf{B}$ heating.
- Maxwell-J$\ddot{u}$ttner distribution
- Temperature scales with:

$$T(MeV) = 0.511\left(\sqrt{1 + \frac{I_{18}\lambda^2_{\mu m}}{1.37}} - 1\right)$$

- Propagate through the target
- Generation of Electric and Magnetic Fields

What are Fast Electron Beams?

- Generated from $\mathbf{j} \times \mathbf{B}$ heating.
- Maxwell-J$\ddot{u}$ttner distribution
- Temperature scales with:
  $T(MeV) = 0.511\left(\sqrt{1+\frac{I_{18}\lambda_{\mu m}^2}{1.37}}-1\right)$
- Propagate through the target
- Generation of Electric and Magnetic Fields
- Current Neutrality ($j_f \approx -j_B$)

What are Fast Electron Beams?

- Generated from $\mathbf{j} \times \mathbf{B}$ heating.
- Maxwell-J*ü*ttner distribution
- Temperature scales with:
$$T(MeV) = 0.511\left(\sqrt{1+\frac{I_{18}\lambda_{\mu m}^2}{1.37}}-1\right)$$
- Propagate through the target
- Generation of Electric and Magnetic Fields
- Current Neutrality ($j_f \approx -j_B$)
- Return current leads to ohmic heating of the target

Current Work on fast electron transport

Current Work on fast electron transport

- Reduction of the fast electron radius

Current Work on fast electron transport

- Reduction of the fast electron radius
  - Resistive guiding:

Resistive Guiding

$$\frac{\delta \mathbf{B}}{\delta t} = \eta \nabla \times \mathbf{j}_f + \boxed{\nabla(\eta) \times \mathbf{j}_f} \tag{1}$$

Current Work on fast electron transport

- Reduction of the fast electron radius
  - Resistive guiding:

Resistive Guiding

$$\frac{\delta \mathbf{B}}{\delta t} = \eta \nabla \times \mathbf{j}_f + \nabla(\eta) \times \mathbf{j}_f \quad (1)$$

- How fast-electron based heating scales with key experimental parameters

Fast electron heating

Fast electron heating

- Fast electron heating makes a large assumption: a Spitzer like resistivity

Fast electron heating

- Fast electron heating makes a large assumption: a Spitzer like resistivity

$$T \propto \frac{\beta^{\frac{4}{5}} I_L^{\frac{2}{5}} t_h^{\frac{2}{5}}}{\lambda^{\frac{4}{5}} n_i^{\frac{2}{5}}}. \tag{2}$$

Fast electron heating

- Fast electron heating makes a large assumption: a Spitzer like resistivity

$$T \propto \frac{\beta^{\frac{4}{5}} I_L^{\frac{2}{5}} t_h^{\frac{2}{5}}}{\lambda^{\frac{4}{5}} n_i^{\frac{2}{5}}}. \quad (2)$$

- While this is an accurate representation of a plasma, it does not clearly represent the cold target.

Another alternative

Another alternative

- By treating the target via cold resistivity, it is possible to arrive at two different resistivities:

Another alternative

- By treating the target via cold resistivity, it is possible to arrive at two different resistivities:
- Constant resitivity:

$$T \propto \frac{\beta^2 I_L \tau_L}{Z n_i \lambda_L} \tag{3}$$

Another alternative

- By treating the target via cold resistivity, it is possible to arrive at two different resistivities:
- Constant resitivity:

$$T \propto \frac{\beta^2 I_L \tau_L}{Z n_i \lambda_L} \tag{3}$$

- Square root resistivity:

$$T \propto \frac{\beta^4 I_L^2 \tau_L^2}{Z^2 n_i^2 \lambda_L^2} \tag{4}$$

Another alternative

- By treating the target via cold resistivity, it is possible to arrive at two different resistivities:
- Constant resitivity:

$$T \propto \frac{\beta^2 I_L \tau_L}{Z n_i \lambda_L} \tag{3}$$

- Square root resistivity:

$$T \propto \frac{\beta^4 I_L^2 \tau_L^2}{Z^2 n_i^2 \lambda_L^2} \tag{4}$$

- The aim of this work is to preform simulations on a variety of targets to see which model is best suited towards it.

Outline

ZEPHYROS

- ZEPHYROS - Hybrid-PIC code

ZEPHYROS

- ZEPHYROS - Hybrid-PIC code
- Follows Davies(2002) rigid beam model

ZEPHYROS

- ZEPHYROS - Hybrid-PIC code
- Follows Davies(2002) rigid beam model
- Calculates electric field from resistive Ohms Law and by considering current neutrality can arrive at equations for the Electric and Magnetic fields.
- $\mathbf{E} = -\eta \mathbf{j}_f + \frac{\eta}{\mu_0} \nabla \times \mathbf{B}$
- $\frac{\delta \mathbf{B}}{\delta t} = \eta \nabla \times \mathbf{j}_f + \nabla(\eta) \times \mathbf{j}_f + \frac{\eta}{\mu_0} \nabla^2 \mathbf{B} - \frac{1}{\mu_0} \nabla \eta \mathbf{B}$

ZEPHYROS

- ZEPHYROS - Hybrid-PIC code
- Follows Davies(2002) rigid beam model
- Calculates electric field from resistive Ohms Law and by considering current neutrality can arrive at equations for the Electric and Magnetic fields.
- $\mathbf{E} = -\eta \mathbf{j}_f + \frac{\eta}{\mu_0} \nabla \times \mathbf{B}$
- $\frac{\delta \mathbf{B}}{\delta t} = \eta \nabla \times \mathbf{j}_f + \nabla(\eta) \times \mathbf{j}_f + \frac{\eta}{\mu_0} \nabla^2 \mathbf{B} - \frac{1}{\mu_0} \nabla \eta \mathbf{B}$
- Manually enter a resistivity model

ZEPHYROS(II)

Simulation Setup i

- $200 \times 200 \times 200$ grid used with cells being 0.1μm in length.

ZEPHYROS(II)

Simulation Setup i

- $200 \times 200 \times 200$ grid used with cells being 0.1μm in length.
- 4×10^7 particles

ZEPHYROS(II)

Simulation Setup i

- $200 \times 200 \times 200$ grid used with cells being 0.1μm in length.
- 4×10^7 particles
- Initial Parameters followed Taranis laser parameters

ZEPHYROS(II)

Simulation Setup i

- $200 \times 200 \times 200$ grid used with cells being 0.1μm in length.
- 4×10^7 particles
- Initial Parameters followed Taranis laser parameters
- Beam radius of 10μm.

ZEPHYROS(II)

Simulation Setup i

- $200 \times 200 \times 200$ grid used with cells being 0.1μm in length.
- 4×10^7 particles
- Initial Parameters followed Taranis laser parameters
- Beam radius of 10μm.
- Angle of Divergence: 60°(1.047rad).

ZEPHYROS(II)

Simulation Setup i

- $200 \times 200 \times 200$ grid used with cells being 0.1μm in length.
- 4×10^7 particles
- Initial Parameters followed Taranis laser parameters
- Beam radius of 10μm.
- Angle of Divergence: 60°(1.047rad).
- β =of 0.4

ZEPHYROS(II)

Simulation Setup i

- $200 \times 200 \times 200$ grid used with cells being 0.1μm in length.
- 4×10^7 particles
- Initial Parameters followed Taranis laser parameters
- Beam radius of 10μm.
- Angle of Divergence: $60^\circ(1.047\text{rad})$.
- β =of 0.4
- Laser Pulse duration of 5.6×10^{-13}s.

ZEPHYROS(II)

Simulation Setup i

- $200 \times 200 \times 200$ grid used with cells being 0.1μm in length.
- 4×10^7 particles
- Initial Parameters followed Taranis laser parameters
- Beam radius of 10μm.
- Angle of Divergence: 60°(1.047rad).
- β =of 0.4
- Laser Pulse duration of 5.6×10^{-13}s.
- Targets used: Al, Ti, Au & CH

ZEPHYROS(III)

Simulation Setup ii

Run	I(Wcm^{-2})	λ(μm)	n_i(cm^{-3})	Fast e- Temp (MeV)
A	2×10^{19}	1.053	See table 2	1.61
B	9.25×10^{19}			
C	5.55×10^{19}			
D	3.33×10^{19}			
E	1.2×10^{19}			
F	7.2×10^{18}			
G	4.32×10^{18}			
H		4.875		9.02
I		2.925		5.22
J		1.755		2.95
K		0.6318		0.824
L		0.379		0.388
M		0.227		0.166
N			See table 2	
O			See table 2	
P			See table 2	
Q			See table 2	
R			See table 2	
S			See table 2	

ZEPHYROS(IV)

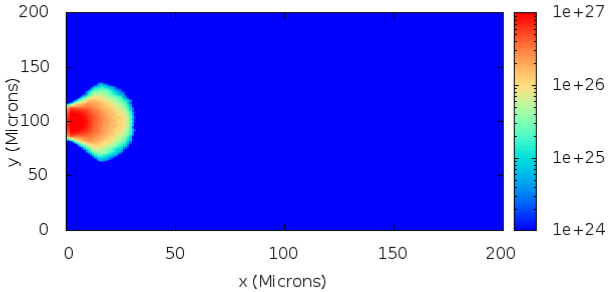
200
150
100
50
0
y (Microns)
0
50
100
150
200
x (Microns)
1e+27
1e+26
1e+25
1e+24

Outline

Heating Profiles

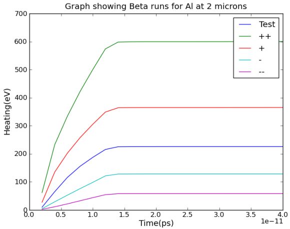

1. Can be seen from the 3 figures that the heating profiles are consistent.

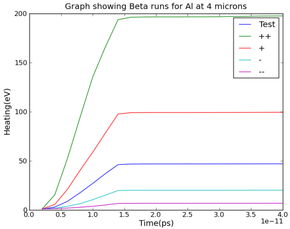

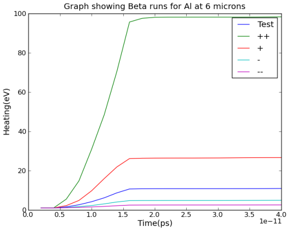

Heating at $2\mu m$

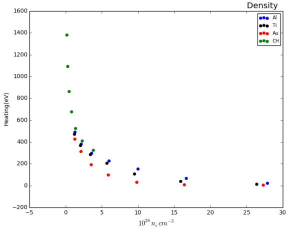

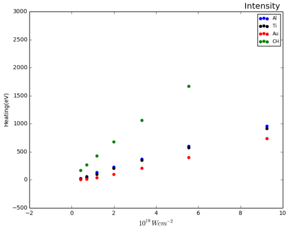

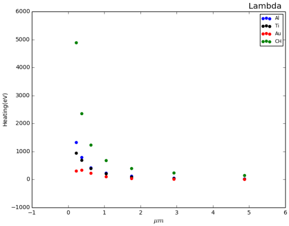

Heating(II)

2 μm

$$T \propto \frac{\beta^{\frac{4}{5}} I_L^{\frac{2}{5}} t_h^{\frac{2}{5}}}{\lambda^{\frac{4}{5}} n_i^{\frac{2}{5}}}$$

$$T \propto \frac{\beta^2 I_L \tau_L}{Z n_i \lambda_L}$$

$$T \propto \frac{\beta^4 I_L^2 \tau_L^2}{Z^2 n_i^2 \lambda_L^2}$$

Run	I	λ	n_i
Al	1.17037	1.3973	0.9461
Ti	1.31882	1.4853	1.1457
Au	1.71775	1.6205	1.6167
CH	0.89455	1.1440	0.4761

Heating(III)

4 μm

$$T \propto \frac{\beta^{\frac{4}{5}} I_L^{\frac{2}{5}} t_h^{\frac{2}{5}}}{\lambda^{\frac{4}{5}} n_i^{\frac{2}{5}}}$$

$$T \propto \frac{\beta^2 I_L \tau_L}{Z n_i \lambda_L}$$

$$T \propto \frac{\beta^4 I_L^2 \tau_L^2}{Z^2 n_i^2 \lambda_L^2}$$

Run	I	λ	n_i
Al	1.54547	1.74238	1.35978
Ti	1.71326	1.74842	1.48347
Au	1.71396	1.31961	1.61393
CH	0.89452	1.14852	0.49701

Heating(IV)

6 μm

$$T \propto \frac{\beta^{\frac{4}{5}} I_L^{\frac{2}{5}} t_h^{\frac{2}{5}}}{\lambda^{\frac{4}{5}} n_i^{\frac{2}{5}}}$$

$$T \propto \frac{\beta^2 I_L \tau_L}{Z n_i \lambda_L}$$

$$T \propto \frac{\beta^4 I_L^2 \tau_L^2}{Z^2 n_i^2 \lambda_L^2}$$

Run	I	λ	n_i
Al	1.41015	1.29582	1.35218
Ti	1.52150	1.36827	1.34533
Au	1.23550	0.60065	1.2817
CH	0.88295	1.11727	0.50418

Strong Heating Limit

$$T \propto \frac{\beta^{\frac{4}{5}} I_L^{\frac{2}{5}} t_h^{\frac{2}{5}}}{\lambda^{\frac{4}{5}} n_i^{\frac{2}{5}}}$$

$$T \propto \frac{\beta^2 I_L \tau_L}{Z n_i \lambda_L}$$

$$T \propto \frac{\beta^4 I_L^2 \tau_L^2}{Z^2 n_i^2 \lambda_L^2}$$

Run	I	λ	n_i
Al(10eV)	1.17037	1.3973	0.9461
Al(50eV)	1.06293	1.1934	0.7301
Al(100eV)	0.96880	1.1934	0.5593
Ti(10eV)	1.4308	1.4853	1.6153
Ti(50eV)	1.07748	1.177	0.6947
Ti(100eV)	0.97502	1.0041	0.6947
Au(10eV)	1.60688	1.1132	1.2631
Au(50eV)	1.31637	0.7412	0.9605
Au(100eV)	1.24259	0.2969	0.7802

Conclusion

- Assumed Spitzer resistivity for solid targets has shown to be an incorrect assumption

Conclusion

- Assumed Spitzer resistivity for solid targets has shown to be an incorrect assumption
- Results show that these targets are far better modelled via a cold temperature resistivity.

Questions?